CHAPTER 252

Observed Suspended Sediments in Storm Conditions

J.J. Williams[1], C.P. Rose[2], P.D. Thorne[1], L.E. Coates[2], J. R. West[2], P.J. Harcastle[1], J.D. Humphery[1], S.P. Moores[1] & D. J. Wilson[1]

Abstract

High resolution synchronous measurements of turbulence, waves and vertical suspended sediment (S_{sed}) concentration profiles have been obtained during a storm above a rippled bed comprising coarse/medium sand located close to the end of a large offshore sand bank in a water depth of approximately 20m. These data are utilised to study the temporal characteristics of sediments in suspension. Sediment resuspension 'events', exhibiting vertical coherence up to approximately 30cm above the sea bed, are observed to span a range of temporal scales encompassing half wave, wave and wave group periods. The vertical concentration of S_{sed} is shown to be enhanced significantly by wave groups. Average S_{sed} profiles are described using a simple Rouse-type and an new 'convective' model.

Introduction

At the most fundamental level, a fluid motion directed away from the bed with a velocity exceeding the *in situ* grain settling velocity is the basic requirement for the suspension of sediments. In marine situations, such fluid motion can arise in three ways (*Pykhov et al., 1995*): (a) turbulent fluid '*bursting*' (*Kline et al., 1967; Hino et al., 1983; Sleath, 1987*); (b) vortices formed by interactions between waves, currents and the bed (*Mogridge & Kamphuis, 1972; Kaneko, 1981*); and (c) vortices formed under breaking waves which penetrate to the bed (*Nadaoka & Kondoh, 1989*). Spatial and temporal scales determined by the hydrodynamics and the physical properties of the sediment makes simple descriptions of the instantaneous physical characteristics of suspended sediment difficult and most approaches consider only time-average conditions. Further, in field situations, waves at angles to tidal currents frequently lead to the generation of complex and interacting bedform assemblages (*Sleath, 1984*) adding further complexity to the modelling of sediment dynamics.

---

1 Proudman Oceanographic Laboratory, Bidston Observatory, Birkenhead, Merseyside, L43 7RA, UK, (*jjw@pol.ac.uk*).

2 School of Civil Engineering, The University of Birmingham, Edgbaston, Birmingham, B15 2TT, UK.

Recently, the use of acoustic instruments has enabled acquisition of high temporal resolution data pertaining to the vertical distribution of suspended sediment in marine conditions (e.g. *Thorne et al., 1993*; *Lee & Hanes, 1996*) and progress has been made in understanding and modelling of sediment resuspension and suspension dynamics. However, the majority of experiments examining sediment processes in marine situations have been conducted just outside the breaker zone in moderate conditions (e.g. *Osborne et al., 1994*) and few field data relate to the mobilisation of sediments during storm conditions at offshore locations (e.g. *Green et al., 1995*). As a consequence, data necessary for validation of numerical models of sediment transport in extreme conditions remains scarce. The present paper presents field observations of suspended sediments and hydrodynamic conditions in the first metre of the water column above a rippled coarse/medium sandy bed in a water depth of 20m during a moderate storm.

Field site and measurements

The study site was located close to the northern end of Middelkerke Bank in the Flemish sand banks, southern North Sea, Europe (*Figure 1a*). Middelkerke Bank is approximately 10km long, 1-2km wide and is located approximately 10km offshore. Bottom sediments consisted of medium/coarse sand (D_{50} = 450μm). Approximately 15% of the sediment by weight was composed of platy angular shell fragments (D_{50} = 650μm). Data relating to hydrodynamic conditions (turbulence and waves) and vertical suspended sediment concentration (S_{sed}) profiles have been obtained using the autonomous benthic lander *STABLE* (*Figure 1b*, *Humphery & Moores, 1994*).

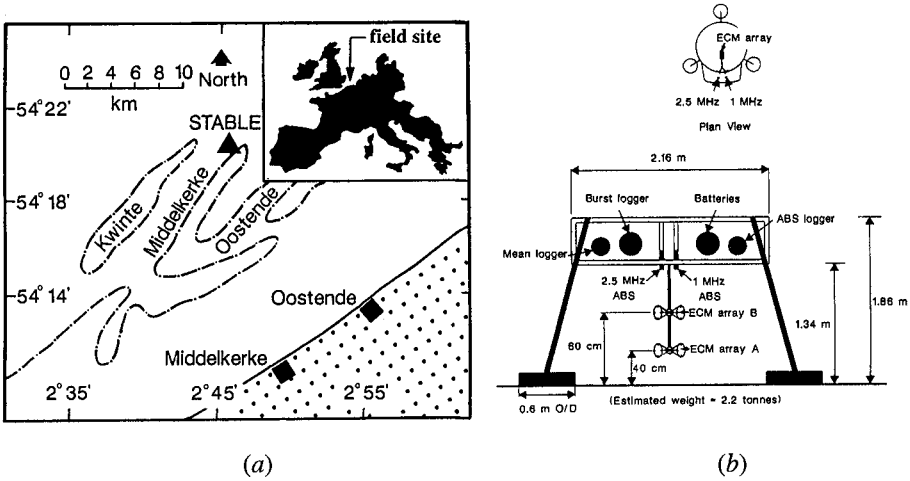

(*a*) (*b*)

Figure 1. (a) Location of the field site at Middelkerke Bank, Belgium; (b) *STABLE* (Sediment Transport And Boundary Layer Equipment).

Instantaneous near-bed flow in orthogonal vertical planes (x-z, y-z) was measured using pairs of electromagnetic current meters (*ECM*, diameter 10cm) at heights (z) of approximately 36cm and 76cm above the sea bed (*Figure 1b*). A pressure sensor at z = 1.63m was used to measure waves. *ECM* and wave data were sampled at 8Hz for approximately 19 minutes every hour in '*burst*' mode. The analysis methods used to obtain hydrodynamic parameters referred to below are described by *Hannay et al., (1994)*. A vertical profile of S_{sed} perpendicular to the *ECM*'s over the range 1cm < z < 100cm with a vertical resolution of 1cm was derived from two acoustic backscatter sensors (*ABS*) operating at 1.0MHz (*ABS1*) and 2.5MHz (*ABS2*), (*Thorne et al., 1993*). These sensors were separated horizontally by a distance of 10cm along a line normal to the *ECM* axis (*Figure 1b*) and were synchronised precisely with *ECM* and pressure sensor data. *ABS* data were recorded independently in *burst* mode at 4Hz for approximately 9 minutes every hour. *ABS* data were calibrated in the laboratory using samples of the bed sediments from the *STABLE* deployment site (*Wylie et al., 1994*). For the range of instantaneous and average S_{sed} values observed in the present study ($\approx 10^{-4}$ - 10^{1}g/l), close agreement was found between *ABS1* and *ABS2*. Estimates of ripple wavelength ($\lambda \approx$ 50cm) were obtained in the field using the *ABS* instruments and ripple height (a) was estimated using an empirical relationship between ripple steepness and grain Shields number (*Nielsen, 1981*) and approximated to 7cm. The physical roughness (k_s) of the ripples was calculated using $k_s = 8a^2/\lambda$, (*Nielsen, 1992*).

Experimental conditions

In total 50 *burst* records encompassing calm and storm conditions were obtained. A detailed description of the hydrodynamic conditions occurring during the periods preceding and following the storm is given by *Williams et al., (1996)*. In the present paper attention is focused upon a period of 5 hours spanning the peak of storm activity (*bursts* 34-39) when the average S_{sed} value reached a maximum. *Burst* average hydrodynamic conditions and S_{sed} values observed during this period are summarised in *Figure 2*.

During *bursts* 34-39, wave direction ($\psi_w \approx 330^o$) and current direction ($\psi_c \approx 200^o$) remained approximately constant and *burst* average S_{sed} values increased in response to increasing tidal current speed and wave orbital speed (*Figure 2*). Following *burst* 38, S_{sed} values decreased as the storm subsided. During the storm, waves were observed to be long-crested and groupy in nature and the vertical position of the bed was observed to change relative to *ABS* sensors. Since the motion sensors on *STABLE* indicated that the rig remained static during the experiment it is considered likely that the observed changes in bed elevation are attributable to the migration of bedforms beneath *STABLE*.

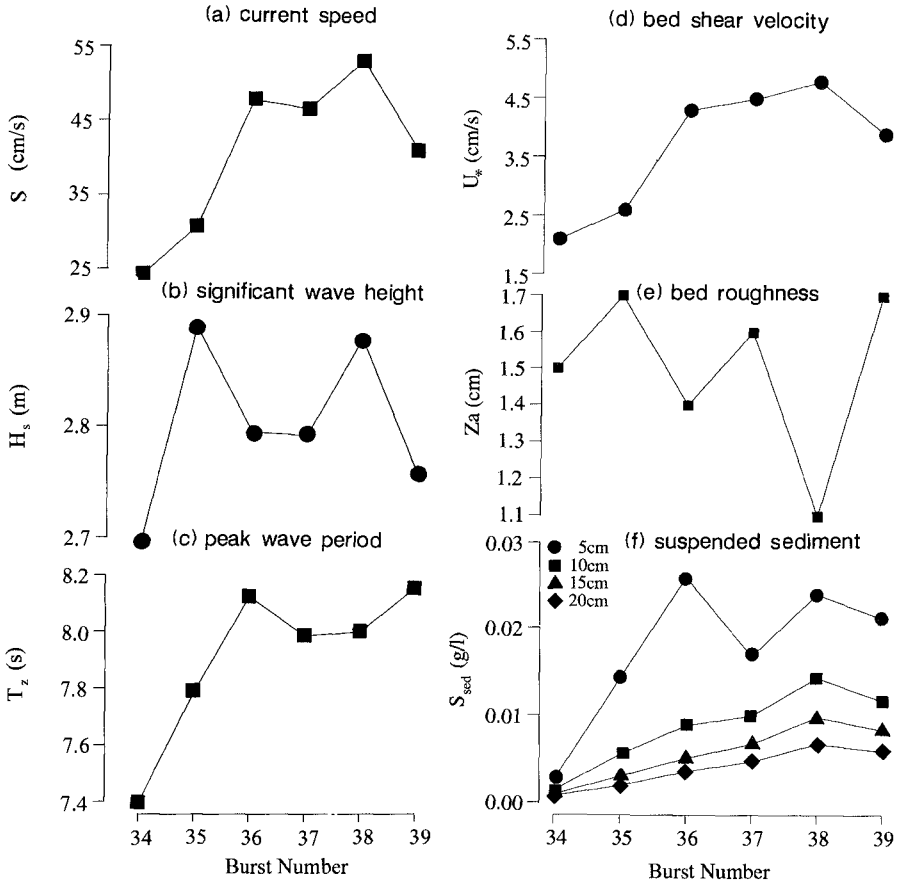

Figure 2. (a) *burst* average current speed (S) at z = 76cm ; (b) significant wave height (H_s); (c) peak wave period (T_p); (d) *burst* average bed shear velocity (currents) obtained using the turbulent kinetic energy (t.k.e.) method (*cf. Hannay et al., 1994*); (e) apparent bed roughness (z_a); and (f) S_{sed} at z = 5-20 cm.

Results and discussion

Observed temporal and spatial structure of sediment resuspension events

Typical time series measurements of S_{sed} at z = 4cm, 6cm, 10cm and 40cm and surface wave amplitude are shown in *Figure 3*. S_{sed} time series in this *figure* comprise a 'background' population of suspended material ($\approx$ 0.02g/l at z = 4cm) and

discrete resuspension *events* in which instantaneous S_{sed} peaks frequently exceed 1.0g/l. Whilst *Figure 3* shows strong visual correlation between waves and S_{sed} *events* and marked vertical coherence in S_{sed}, coherent vertical fluid motion necessary to suspend sediment was not detected by the *ECM* sensors. This is attributed to the dissipation of coherent vertical fluid motion by $z = 40$ cm and to the physical size of the *ECM* measuring volume.

When examining *Figure 3* it is important to remember that during the storm, long-crested waves were approximately normal to the tidal currents and that the location of the *ABS* sensors changed in relation to ripple crests through time as ripples migrated. However, if it is assumed that resuspension *events* occurred along a significant length of the rippled bed parallel to the wave crests, (i.e. vortices formed by wave action are also long-crested), then material in suspension will be advected past the *ABS* sensors by the combined action of waves and the tidal current as coherent clouds approximately in phase with the waves.

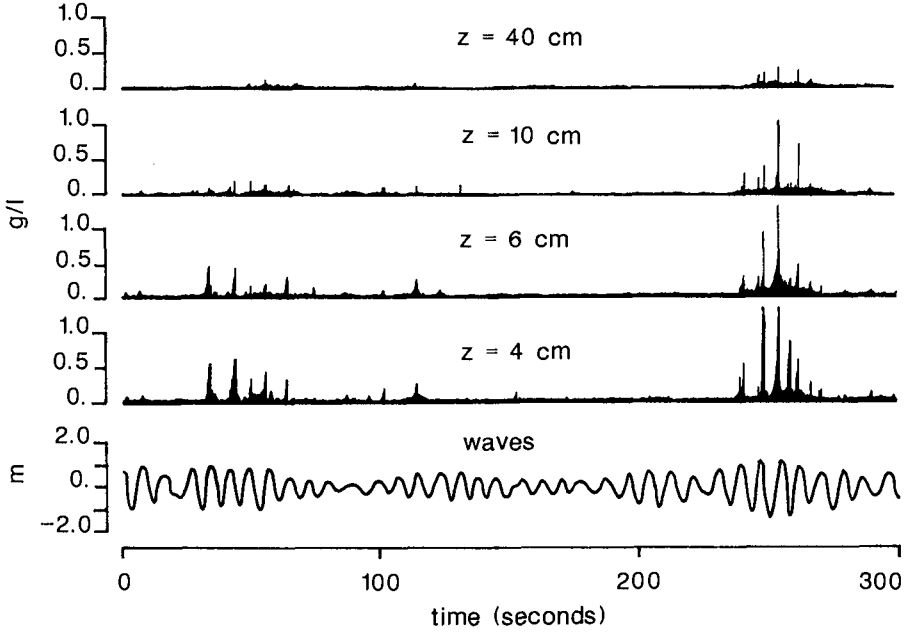

Figure 3. Time series of observed suspended sediments and waves.

Surprisingly, given the strong visual correlation between waves and resuspension *events* illustrated in *Figure 3*, periodic components at wave frequencies were not identified in power spectra of S_{sed} time series irrespective of the observation height above the sea bed. This is attributed to two problems: (i) the S_{sed} time series are 'spiky' in nature; and (ii) the temporal changes in spatial location between *ABS*

sensors and resuspension *event* sources (i.e. ripple crestlines) and spatial variation in horizontal S_{sed} values combine with advected populations of suspended material to results in complex phase relationships between observed surface waves and S_{sed} time series. However, velocity^2-sediment cospectra (*Figure 4*) show statistically significant correlation's between the horizontal flow components squared (u^2 and v^2) and S_{sed}.

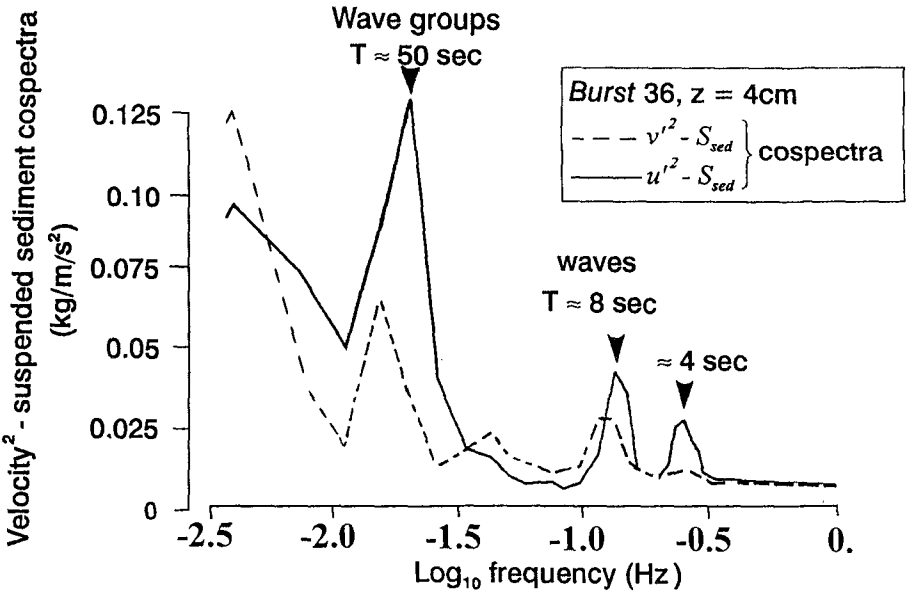

Figure 4. Velocity^2-sediment cospectra, *burst* 38.

Figure 4 shows correlation's between u^2 and S_{sed} and between v^2 and S_{sed} at half wave (≈0.25Hz), wave (≈0.125Hz), wave group (≈0.01Hz) and lower frequencies (in the range 0.01 - 0.003Hz). In all cases examined during the storm, wave groups dominate the cospectra. This is also illustrated visually in *Figure 3*. Although low frequency fluid motion is recorded by *ECM* sensors, it is unclear whether or not the low frequency peak in the velocity^2-sediment cospectra is a real phenomenon or simply an artefact of the analysis method. If shown to be real, further work is then required to quantify the role of this low frequency component in suspended sediment transport.

Waves recorded during *bursts* 34-39 exhibited well developed groupy structure (*Figure 3*). Initial visual inspection of correlation's between the wave groups and modulation in suspended sediment concentration indicated strongly that successive waves in a group resulted in a progressive increase in average S_{sed} values up to $z \approx$ 30 cm consistent with the idea of *wave pumping*. It was also determined that average

S_{sed} values associated with the last wave in a given group of more than 6 waves were a factor of approximately 2 times larger than values associated with the first wave in the same group. Following passage of a group, average S_{sed} values were observed quickly to decline to their former value.

In order to investigate further the wave-by-wave 'pumping' effect, the Goda run-length was utilised (*Goda, 1985*). Here, the start of a wave group was defined by the passage of a wave of height (h_j) that was observed to mobilise bottom sediments. For the group to continue, successive waves must be equal to or exceed h_j. In all cases an observed linear increase in average S_{sed} values with j demonstrated the enhancement of the sediment resuspension process by the passage of a successive series of larger than average waves (*Figure 5*). At present suspended sediment transport formulae do not include explicitly this important effect and thus are likely to underestimate the sediment transport rate in combined wave-current situations.

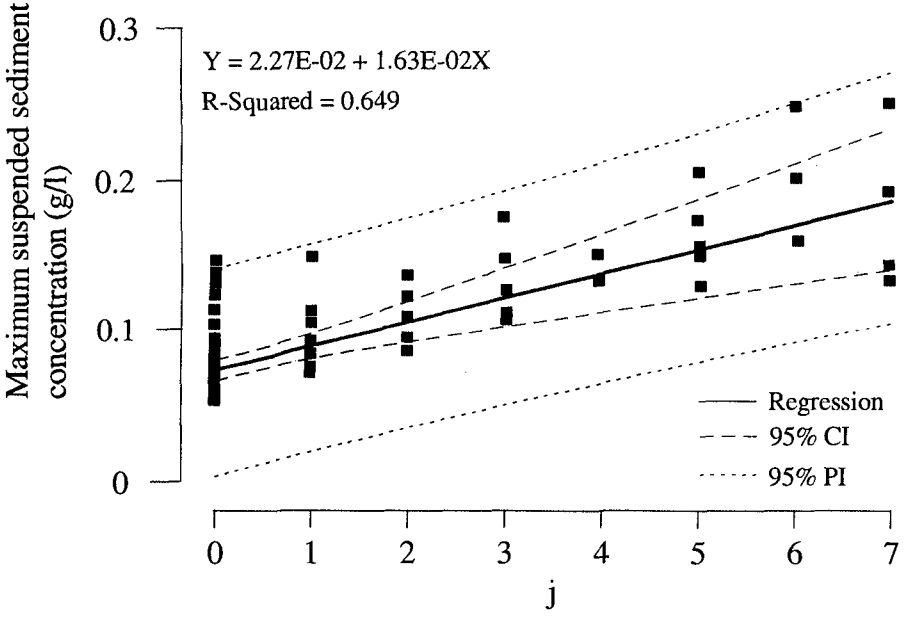

Figure 5. Goda wave group run length (j) versus observed suspended sediments.

Burst average suspended sediment concentration profiles

Burst average suspended sediment concentration profiles observed over the range 1cm < z < 50cm are shown in *Figure 6*. Since ripples are observed to migrate beneath the *ABS* sensors during a *burst* measurement period, these profiles also represent horizontally spatially averaged S_{sed} values in the direction of ripple migration. The observed profiles show a progressive increase in the *burst* average

suspended sediment concentration over the range 1cm < z < 50cm from a minimum during *burst* 34 to a maximum during *burst* 38. At z > 50cm, S_{sed} values are small (0.001g/l to 0.005g/l) and slowly decay with height above the bed. In all cases the profiles are smooth, continuous and are Rouse-like above z ≈ 20cm. In the bottom 10cm, S_{sed} profiles for *bursts* 37-39 exhibits a significant concave curvature which develops through the storm.

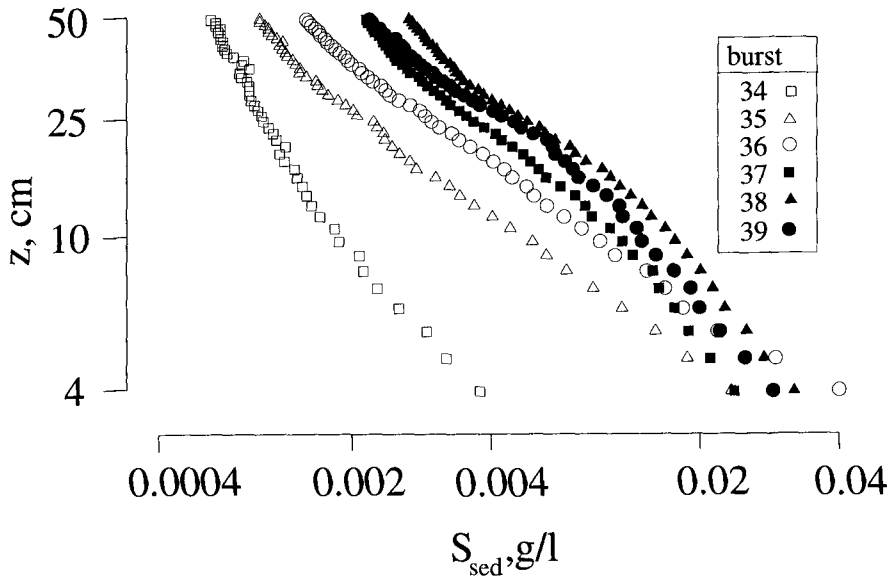

Figure 6. Suspended sediment concentration profiles, *bursts* 34-39.

During the period of increasing wave height preceding the peak storm activity, S_{sed} profiles in the range 3cm < z < 40cm for *bursts* 34-36 were found to follow approximately Rouse-type profiles defined by *Smith (1977)* as

$$C(z) = C(a)(z/a)^{-\alpha} \qquad (1)$$

where α is the Rouse parameter (i.e. $\alpha = w_s / \beta\kappa U_{*wc-max}$), $C(z)$ and $C(a)$ are S_{sed} values at heights z and a, respectively, above the sea bed, w_s is the settling velocity (estimated to be 3.5 cm/s, *van Rijn, 1989*), β is the ratio of the eddy diffusion coefficients for the fluid and the sediment (assumed to be 1.0), κ is the von Kármán coefficient (0.4) and $U_{*wc-max}$ is the maximum wave-current bed shear velocity.

Using a least squares fit to the straight line portion of the observed S_{sed} profiles, values for α were obtained from the gradient of the straight line fit, (*Table 1*).

Burst	S (cm/s)	σ_w (cm/s)	α	$U_{*wc-max}$ (cm/s)
34	24.2	15.5	1.27	-
35	30.9	20.7	1.32	6.6
36	47.8	22.7	1.33	6.6

Table 1. S, RMS wave orbital speed σ_w, α and $U_{*wc-max}$, values derived from observed S_{sed} profiles (*Eq. 1*), *bursts* 34-36.

Utilisation of the observed α values in *Eq. 1* gave predicted S_{sed} values that matched well observed S_{sed} values for *bursts* 34-36 ($R^2 > 0.95$). $U_{*wc-max}$ values for *bursts* 35 and 36 agree broadly with values predicted by a number of wave-current models (e.g. *Soulsby, 1994*). Although S and σ_w values measured during *burst* 34 are significantly lower than those pertaining during *bursts* 35 and 36, a larger than expected value for $U_{*wc-max}$ was obtained from the *burst* 34 S_{sed} profile data (6.8cm/s). This may imply that the assumed settling velocity of 3.5 cm/s is incorrect for this *burst* and for this reason the value for $U_{*wc-max}$ for *burst* 34 is not included in *Table 1*.

In the case of *bursts* 37, 38 and 39 a new expression is required to simulate the concave curvature in the bottom 10cm of the observed profiles (*Figure 6*). In these cases it was found that the whole S_{sed} profile for 1 cm $< z <$ 40 cm could be matched closely to the "convective" empirical profile proposed by *Nielsen (1992)* for natural sand ripples composed of coarse grains in oscillatory flows. Thus

$$C(z) = C(0)\left(\frac{z}{L} + 1\right)^{-\alpha'} \qquad (2)$$

where L is a characteristic length scale. *Nielsen (1992)* suggests a value of 2 for α'. In contrast to *Eq. 1*, *Eq. 2* tends towards a Rouse-type profile when $z/L >> 1$ and also tends toward $C(0)$ at the bed. The gradients of S_{sed} profiles depart from the form of *Eq. 2* at z > 30-40cm where finer material in suspension might be anticipated. Present data indicates that the vertical distribution of S_{sed} in the range 35cm $< z <$ 100cm can be modelled well using a second Rouse-type profile with a smaller α value. However, for $z >$ 50cm, S_{sed} values are observed to be 3-4 orders of magnitude

less than those observed at z < 10cm and can therefore be neglected for practical purposes when estimating rates of sediment transport.

In the present study, *Eq. 2* was obtained using a semi-analytical approach by assuming that the total wave-current sediment diffusivity is the sum of the Rouse-type diffusivity defined in *Smith (1977)* and a constant diffusivity (ε_c) found in oscillatory only flow over ripples (*Nielsen, 1992*). This gives

$$-w_s C = \left(\kappa U_{*wc-max} z + \varepsilon_c\right)\frac{\partial C}{\partial z} \qquad (3)$$

and hence

$$C(z) = C(a)\left(\frac{z+L}{a+L}\right)^{-\alpha'} \qquad (4)$$

where α' is a Rouse-type parameter and $L = \varepsilon_c / \kappa U_{*wc-max}$. When $a = 0$, this profile is identical to *Eq. 2*.

The values of the parameters used in *Eq. 4* to obtain the best fit between observed and predicted S_{sed} profiles for *bursts* 37-39 are shown in *Table 2*. These were obtained by firstly estimating the gradient of the straight line portion of a given S_{sed} profile (α') on log-log axes (typically this fell within the range 15cm < z < 25cm). Using the suspended sediment concentration values at z = 4cm as a 'reference' concentration, values of L were obtained using $C(z)$ values up to z = 25cm. Finally, taking the average value of L (*Table 2*), $C(0)$ was calculated using observed concentration values at z = 4cm and $U_{*wc-max}$ values were derived from α' assuming w_s = 3.5cm/s (*van Rijn, 1989*). A comparison between computed and observed S_{sed} profiles is illustrated in *Figure 7*. In all cases the fit between observed and predicted S_{sed} profiles is statistically significant (R^2 >0.97).

Burst	S (cm/s)	σ_w (cm/s)	$C(0)$ (g/l)	α' –	L (cm)	k_s (cm)	$U_{*wc-max}$ (cm/s)
37	46.6	21.8	0.058	1.27	4.2	7.3	6.9
38	53.1	22.1	0.090	1.48	5.6	10.1	5.9
39	41.0	23.5	0.079	1.29	3.7	13.3	6.8

Table 2. S, σ_w and *Eq. 4* parameter values derived from observed hydrodynamics and S_{sed} profile data, *bursts* 37-39.

Table 2 shows that values for α' are lower than the value suggested *by Nielsen (1992)* and are similar to the α values shown in *Table 1* suggesting α' may be the same parameter. Values of the parameter L in the range 3.7-5.6 are only a factor of two to four times lower than k_s values. A relationship between these two parameters is therefore suggested. Work to improve the fit between observed and predicted S_{sed} profiles for these and other field observations of suspended sediment profiles in marine situations is currently being undertaken by the authors.

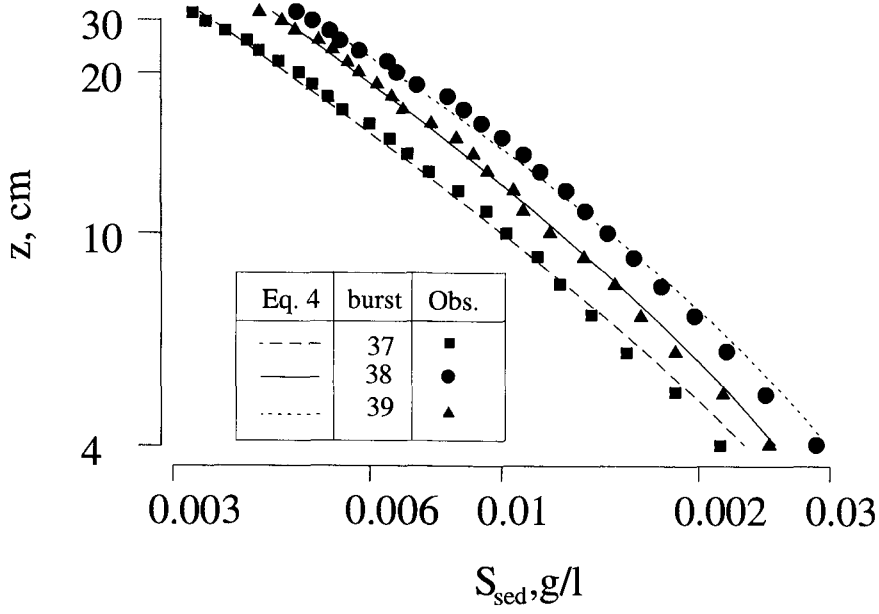

Figure 7. Comparison between and computed S_{sed} profiles, *bursts* 37-39.

Conclusions

(i) Field data have been obtained in the bottom 1m of the water column during a storm.

(ii) Present analysis has examined the temporal response of medium/coarse sandy sediments to waves and tidal currents.

(iii) Sediment resuspension has been shown to be enhanced significantly by the passage of groups of waves.

(iv) Average S_{sed} profiles observed during storm conditions have been represented using a 'simple' Rouse-type profile (*Smith, 1977*) and a new wave-current profile based upon the "convective" empirical profile proposed by *Nielsen (1992)*. The new profile allows accurate determination of *C(0)*.

Acknowledgements

This work was funded jointly by NERC and by The Commission of the European Communities Directorate General for Science and Education, Research and Development under contract number MAS2-CT-0024 (CSTAB).

References

GODA Y (1985) Random sea and design of maritime structures. University of Tokyo Press.

GREEN M.O., VINCENT C.E., McCAVE I.N., DICKSON R.R., REES J.M. & PEARSON N.D. (1995) Storm sediment transport: observations from the British North Sea shelf. *Continental Shelf Research*, **15**, 889-912.

HANNAY A., WILLIAMS J.J., WEST J.R. & COATES L.E. (1994). A field study of wave:current interactions over a rippled sandy bed. *EUROMECH 310: Sediment Transport Mechanisms in Coastal Environments and Rivers*, M. Belorgey, R.D. Rajaona & J.A.F. Sleath (editors), World Scientific, 345-359.

HINO M., KASHIWAYANAGI M. & NAKAYAMA A. (1983) Experiment on the turbulence statistics and the structure of a reciprocating oscillatory flow. *Journal of Fluid Mechanics*, **131**, 363-400.

HUMPHERY J.D. & MOORES S.P. (1994) STABLE II - An improved benthic lander for the study of turbulent wave-current-bed interactions and associated sediment transport. *Electronic Engineering in Oceanography*, IEE Conference Publication No. **394**, 170-174.

KANEKO A. (1981) Oscillation sand ripples in viscous fluids. *Proceedings of the Japanese Society of Civil Engineering*, **307**, 113-124.

KLINE S.J., REYNOLDS W.C., SCHRAUB F.A. & RUNDSTADLER P.W. (1967) The structure of turbulent boundary layers. *Journal of Fluid Mechanics*, **30**, 741-773.

LEE T.H. & HANES D.M. (1996) Comparison of field observations of the vertical distribution of suspended sand and its prediction by models. *Journal of Geophysical Research*, **101**, 3561-3572.

MOGRIDGE G.R. & KAMPHUIS J.W. (1972) Experiments on bedform generation by wave action. *Proceedings 13th. Conference on Coastal Engineering*, Vancouver, Canada, 1123-1142.

NADAOKA K. & KONDOH T. (1989) Turbulent flow field structure of breaking waves in the surf zone. *Journal of Fluid Mechanics*, **204**, 359-387.

NIELSEN P. (1981) Dynamics and geometry of wave-generated ripples. *Journal of Geophysical Research*, **86**, 6467-6472.

NIELSEN P. (1992) *Coastal bottom boundary layers and sediment transport*, World Scientific Publishing Co., River Edge, N.J, USA.

OSBORNE P.D., VINCENT C.E. & GREENWOOD B. (1994) Measurement of suspended sand concentrations in the nearshore: field intercomparisons of

optical and acoustic backscatter sensors. *Continental Shelf Research*, **14**, 159-174.

PYKHOV N.V., KOS'YAN R.D. & KUZNETSOV S. YU. (1995) Time scales of sand suspending by irregular waves. *Proceedings of the Second International Conference on the Mediterranean Coastal Environment*, Tarragona, Spain, Vol. **2**, 1073-1092.

SLEATH J.P.A. (1984) *Sea Bed Mechanics*. John Wiley & Sons, 335 pp.

SLEATH J.P.A. (1987) Turbulent oscillatory flow over rough beds. *Journal of Fluid Mechanics*, **182**, 369-400.

SMITH J.D. (1977) Modelling of sediment transport on continental shelves. In: *The Sea*, 6, E.D Goldberg, I.N. McCave, J.J. O'Brien & J.H. Steele (Eds.), Wiley, New York, pp. 539-578.

SOULSBY R.L. (1994) *Manual of Marine Sands*. Report **SR 351**, HR Wallingford, UK, 70pp.

THORNE P.D., HARDCASTLE P.J & SOULSBY R.L. (1993) Analysis of acoustic measurements of suspended sediments. *Journal of Geophysical Research*, **98**, 899-910.

VAN RIJN L.C. (1989) *Handbook Sediment Transport by Currents and Waves*. Delft Hydraulics, Report **H 461** (2^{nd}. edition).

WILLIAMS J.J., THORNE P.D., O'CONNOR B.A., HUMPHERY J.D., HARDCASTLE P.J., MOORES S.P. & COOKE J.A. (1996) Interactions between currents, waves and sediments in calm and storm conditions. *Continental Shelf Research*, (submitted).

WYLIE T., TAYLOR K. & BORN A. J. (1994) Design and calibration of the sediment tower. *POL Internal Document* Number **60**, 15pp, (*unpublished manuscript*).